

Response to Referee #1's Comments

We would like to thank Referee #1 for his/her time, constructive and helpful comments and suggestions.

Major comments

1) Page 22160, line 26 the authors mention that “the “STS+NAT” and “CALIPSO constrained” runs were closer to the measurements than the “STS”run.” According to the legend in figure 8, “STS+NAT” is in black, “CALIPSO constrained” in blue and “STS” in grey. Thus the “STS+NAT” and “STS” runs are closer to the measurements than the “CALIPSO constrained” run. This impacts the conclusion given between page 22160 line 29 and page 22161 line 1. The authors cannot claim that the amount of chlorine activation on PSCs is dependent on PSC classification. Same remark for page 22162 line 24 and in the abstract page 22142 line 20. However, this remark are not such as to call into question the main results of the paper but should be rectified.

You are right. We agree that we cannot claim that the amount of chlorine activation on PSCs is dependent on PSC classification. Also, there is inconsistency between PSC number densities used for “CALIOP constrained” run and other (“STS+NAT” and “STS”) runs, as is pointed out in the following comment 2). This inconsistency comes from different PSC models used for these runs. We discussed on this issue among co-authors, and concluded that it is no use to show these three model run results in the paper, because there is no fundamental differences in the model results to discuss. Therefore, we decided to show only “STS+NAT” model run results throughout the paper.

2) For “STS+NAT” run, the authors use a NAT particle number density of 0.1cm^{-3} while for the “CALIOP constrained” run, they use 10^{-3}cm^{-3} . In a same manner, they use an ice

29 *particle number density of 0.01cm⁻³ while for the “CALIOP constrained” run, they use 1 cm-*
30 *3. In order to better compare the results of the two runs, why do the authors not use the same*
31 *particle number densities?*

32

33 As is stated in the above reply for your comment 1), this difference comes from the different
34 origin of the PSC models. As is stated above, we decided to show only “STS+NAT” model
35 run results throughout the paper.

36

37 *3) The first part of the paper discusses the link between temperature evolution and CALIOP*
38 *PSC composition observation. However, there is no discussion/explanation of why*
39 *temperatures are sometimes below the PSC thresholds and no PSC are observed by CALIOP.*
40 *This is the case in figure 4 (day 4), figure 5a (day 2), figure 5b (day 2), figure 11 (day 2), and*
41 *figure 13 (day 4). This also concerns the second part of the manuscript for cases #02 (day 2)*
42 *and #09 (day 4 morning) where PSC are simulated by the ATLAS model but not observed by*
43 *CALIOP. Some comments should be included in the manuscript to explain these differences.*

44

45 There are several possible reasons for this: A) We have to interpolate the CALIOP PSC
46 measurements to our trajectory locations, which introduces uncertainty, since we don't really
47 know what type of PSC is on the location of the trajectory. B) Uncertainties in the CALIOP
48 measurements and classification. C) Uncertainties in ECMWF temperature. D) Another
49 possible reason is that this could be real: PSC formation is a complicated process that depends
50 e.g. on temperature history. A) is actually discussed in detail in the paper (page 22146, 4-15).
51 B) is discussed in other papers (Pitts et al., 2007, 2009, 2011). C) is also discussed to some
52 extent in the text. The contents of D) is out of focus of this paper.

53

54

55 *Minor comments*

56

57 *1) Page 22146, lines 4-9. Could the authors specify the maximum time difference between*
58 *CALIOP measurements and the trajectory points? For the distance, it is less than 100-200*
59 *km?*

60

61 The maximum time difference is 24 hours. We have added the description ‘closest to each
62 trajectory point “on the same day”’ on page 22146, line 5. You are correct that the distance is
63 typically around 100-200 km. We hope that is implicitly clear from the statement on page
64 22146, line 14-15.

65

66 *2) Figure 2. Could the authors better explain how they get the CALIOP field? As CALIOP*
67 *data are only available where circles are, how the PSC composition between these circles is*
68 *determined? The method detailed page 22147 to get the PSC field is not clear.*

69

70 We have added the description “Global PSC field was created by selecting the closest
71 CALIOP PSC measurement on the same day.” at the end of page 22147, line 18.

72

73 *3) In this study, the authors use the MLS version 3.3. The MLS version 4.2. is now available*
74 *but for HCl and O3, it seems that there are very little or no change compared to V3.3/V3.4*
75 *according to the “version 4.2x Level 2 data quality and description document” (JPL D-33509*
76 *Rev. A). Page 22146, line 22, the authors can mention that they also use H2O data as*
77 *explained page 22153 line 6.*

78

79 At the time when the calculations were made, no version 4.2 data was available. We added
80 H2O as a species on page 22146, line 22.

81

82 *4) Page 22147 line 14, the authors should change “below TNAT“ to “above TNAT”.*

83

84 “below” is correct here. It refers to “period” and not to “sudden stratospheric warming”.

85
86
87
88
89
90
91
92
93
94
95
96
97
98
99
100
101
102
103
104
105
106
107
108
109
110

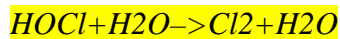
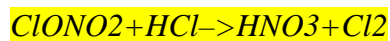
5) Page 22150, lines 3-5, could the authors give a reference for this value of supersaturation needed?

We have added references.

6) Page 22150, line 26, could the authors indicate the value of the assumed supersaturation for HNO₃ over NAT? Is it 10 as mentioned before?

This is the general model description, and the value for the supersaturation is not fixed in the model. Hence, the value is only given in section 4.2, where the actual model setup for the specific runs is described.

7) Page 22155, line 23, to help the reader, the authors should add the reactions :



When the authors mention from page 22143 line 28 to page 22144 line 3 the reaction partner, I suppose that they refer to these reactions.

Thank you for the suggestion. We added these reactions on page 22143, and showed the number of reaction (1) on page 22155.

8) Page 22156, lines 3-5, could the authors indicate why the ATLAS model needs larger spatial and time scales to reproduce HNO₃ measurements?

111 Since the discussion on O₃ and HNO₃ is not essential part of this paper, we deleted all the
112 discussion on O₃ and HNO₃, and related panels from the paper completely.

113

114 *9) For figures 8 to 14, it is necessary to use a 400 % zoom in order to read the figures and see*
115 *the differences between black, grey and blue curves. The authors could probably only focus*
116 *on the part between days -1 and days 5. The figures are very well described in the legend.*
117 *However, explanation about the short backward trajectories observed on figures (d) to (i) is*
118 *missing. I assume that these are the short back trajectories done to find the last model output*
119 *of the global model for chemical initialization. Likewise, on figures 8 to 14 (h), there are*
120 *dotted lines not explained in the legend. I expect it represents the HNO₃ total (gas phase and*
121 *condensed).*

122

123 We need the time axis from -5 to +5 days, since the trajectory is initialized by the MLS
124 measurement of the last 5 days which is described in section 4.3, and these are shown in the
125 plot. The all O₃ and HNO₃ panels are deleted from the paper (see reply to your comment 8).

126

127

Response to Referee #2's Comments

128

129

130

131 We would like to thank Referee #2 for his/her time, constructive and helpful comments and
132 suggestions.

133

134

135 *<General comments:>*

136

137 *The authors examine in their study different topics with the help of several trajectories*
138 *calculated with ATLAS. In my opinion this method is innovative and appropriate for the*
139 *performed study.*

140

141 Thank you very much.

142

143 *From about 30 calculated trajectories, they choose eleven for their study. Unfortunately it is*
144 *not clear, what kind of criteria they use to choose these eleven trajectories. For example*
145 *number 3 and 4 are very similar. That issue should be cleared by the authors.*

146

147 The way of selecting the trajectories is described in Section 3.2 in detail. The selected eleven
148 cases are chosen to cover several different PSC composition classifications and different
149 temperature histories. We agree that case #03 and #04 are rather similar. Therefore, we
150 deleted case #03 from the draft.

151

152 *In the result section 5.1 (with the help of Figs. 5 to 7) Nakajima et al. discuss the dependence*
153 *of PSC classification on their temperature history with the help of CALIOP measurements on*
154 *different chosen trajectories. The authors conclude that the kind of formation of the PSC types*

155 *depends on the temperature history. In cases of rapid temperature decrease first STS is*
156 *formed, followed by NAT/STS clouds. When temperatures dropped below the frost point, ice*
157 *clouds formed, and then transformed into NAT/STS mixture when temperature increase above*
158 *the frost point. This part of the manuscript I find very interesting and the results are in my*
159 *eyes relevant for publication.*

160

161 Thank you very much.

162

163 *In section 5.2 (with the help of the Figs. 8 to 11 and 13) the authors compare the results of the*
164 *ATLAS model with MLS and CALIOP measurements. They performed for this comparison*
165 *three different model runs: “STS+NAT” (I think this is the standard run), “STS” and*
166 *“CALIPSO constrained”.*

167 *The comparison of HCl, and ClO between ATLAS and MLS is in general very good,*
168 *although ATLAS in many cases doesn't match correctly the PSCs from CALIOP and the*
169 *authors can show that chlorine activation is limited by the amount of available ClNO₂.*

170 *But the comparison of HNO₃ fits not very well and the O₃ comparison is difficult because*
171 *there are only small variations in ozone on the selected trajectories. The authors write that*
172 *the ATLAS model cannot reproduce the denitrification for a single trajectory (page 22156,*
173 *line 3-7). In this case I would suggest to skip the HNO₃ and also the O₃ comparisons.*

174

175 We agree that denitrification is difficult to simulate for a single trajectory. Since HNO₃ is not
176 the essential part of this paper, we deleted all the discussion and panels on HNO₃ from the
177 draft. Also, simulated and modeled O₃ depletion on the trajectory is small, because not enough
178 sunlight is available in this period of year. Therefore, we also deleted the discussion and
179 panels on O₃.

180

181 *In general I would also recommend to examine one or two less trajectories studies, because*
182 *there are in my opinion too much similar figures to consider. Maybe it would also be a*
183 *solution to add a supplement with more trajectory cases.*

184

185 We disagree to reviewer's comment on this point. Each trajectory case shown in the draft
186 represents different temperature history and different PSC classification history on the course
187 of trajectory. Therefore, we kept all figures in the current draft.

188

189 *Moreover I don't see really the relevance of the both sensitivity runs ("STS" and "CALIPSO*
190 *constrained"). In my opinion there is no real improvement shown through the results of these*
191 *sensitivity runs. Especially if the setup regarding the number density of NAT and ice particles*
192 *in the "STS+NAT" run and "STS" run is different as in the "CALIPSO constrained" run*
193 *(Sect. 4.2) it should be considered to skip all results of the sensitivity runs from the figures*
194 *and remove the corresponding discussion in the publication.*

195

196 We agree to the reviewer's comment on this point. There is not enough differences between
197 the three sensitivity runs. Moreover, the number densities used for these runs are different,
198 because different PSC scenarios were used for these runs. Therefore, we used only
199 "STS+NAT" run results, and deleted results and sensitivity runs part (Section 4.2) from the
200 draft.

201

202 *In Section 5.3. (with the help of Figs. 12 and 14) Nakajima et al. confirm that the formation of*
203 *PSCs are very temperature dependent with the help of two another sensitivity runs (+1K and -*
204 *1K temperature runs). The authors claims that the run with decreased temperatures fits better*
205 *with the observations. But in my opinion this is at the most valid for HCl. With focus to the*
206 *surface area density, ClO or HNO₃ I don't see really an improvement. The conclusion that*
207 *the formation of NAT is temperature dependent is in my opinion not really new. I would*
208 *suggest also to remove this subsection or at least to choose different trajectories with better*
209 *results.*

210

211 The comparison with HNO₃ is difficult by ATLAS model as is explained above, and we
212 deleted HNO₃ panels from the draft. The purpose of showing Figs. 12 and 14 is to represent

213 that chlorine activation is very sensitive to temperature. Therefore, we keep these figures and
214 discussion in the draft.

215

216

217 *<Specific comments:>*

218

219 *Page 22142, 16-17: In my opinion the ATLAS model results only agree well with the*
220 *observations in the case of HCl and ClO. Please add this here.*

221

222 Since we deleted discussion on HNO₃ from the draft, we think that the current description is
223 OK.

224

225 *22143, 4: If you mention that STS is H₂O-H₂SO₄-HNO₃, perhaps you should also mention*
226 *that NAT is HNO₃(H₂O)₃*

227

228 We added the suggested description there.

229

230 *22143, 21: Voigt et al., 2005 and Hoyle et al., 2013 only assume heterogeneous nucleation of*
231 *NAT on meteoritic dust. Biermann et al., 1996 showed in laboratory experiments that*
232 *heterogeneous nucleation rates on micrometeorites are too low to enhance freezing of polar*
233 *stratospheric clouds above the frost point.*

234

235 We added description on Biermann et al. (1996) there as you suggested.

236

237 *22143, 24: “(and hence strongly on temperature)”.*

238

239 Changed as suggested.

240

241 *22144, 7-8: I don't know if you really can answer the second question with your study. It's*
242 *really difficult to evaluate the sensitivity of chlorine activation or ozone depletion on different*
243 *PSC types with your study. Moreover there is in my opinion no chemical ozone depletion*
244 *shown on your trajectories neither by the simulation results nor in the observations.*

245

246 You are right that it is difficult to study on the difference of chemical ozone depletion to
247 different PSC composition by our current study. We deleted description for ozone from the
248 text.

249

250 *22146, 1-2: What is the reason that you use only three instead of at least four categories (STS,*
251 *Mix1, Mix2 and ice)?*

252

253 Mix1 and Mix2 are the categories both of which include so-called "NAT" PSC. Therefore,
254 we used conventional three PSC categories, STS, NAT, and ice.

255

256 *22147, 6-11: In my opinion you don't have to describe the legend to the figures in the caption*
257 *and in the text.*

258

259 We deleted some sentences from the text.

260

261 *22150, 3: What is the meaning of supersaturation of 10? 10 percent?*

262

263 We have changed "about" to "of a factor of".

264

265 *22150, 7-9: What criteria do you use to choose these eleven trajectories?*

266

267 The way of choosing the eleven trajectories is to cover several different PSC composition
268 classifications and different temperature histories. We added this description in Section 3.2.

269

270 *22150, 22: Please cite Dee et al. 2011 for the ERA-Interim reanalysis.*

271

272 Cited as suggested.

273

274 *22150, 23: . . .are allowed to form in parallel. . . (?)*

275

276 Changed as suggested.

277

278 *22151, 16: . . . the maximum particle number density?*

279

280 The number density is constant. See Wohltmann et al., 2010.

281

282 *22151, 18: . . . of 10 %?*

283

284 See reply to comment to page 22150, 3.

285

286 *22152, 12: Please explain why do you use here a much smaller NAT number density as in the*
287 *“STS” and “STS+NAT” runs?*

288

289 Since the “CALIOP constrained” run used different PSC scenario compared with other (“STS”
290 and “STS+NAT”) runs, their assumed PSC number densities were different. As is pointed out

291 by your General comments, we found that there is not enough differences between the three
292 sensitivity runs, so we decided to show only “STS+NAT” run results in the draft.

293

294 *22152, 15: Here the same: why do you use here 1 cm-3 instead of 0.01 cm-3?*

295

296 Please see the reply above.

297

298 *22154, 3: In table 1 are eleven selected trajectories not nine*

299

300 We discussed nine (now eight, deleted one case in new Fig. 5 following a reviewer’s
301 comment that old case #03 and #04 are very similar) cases from table 1 for PSC evolution by
302 temperature history. Other three cases (#02, #03, and #09) are used for temperature
303 sensitivity study (Figs 11/12, and Figs 13/14).

304

305 *22154, 9: “When temperatures warmed above T_{NAT} in trajectory case #1. . .”*

306

307 Changed as suggested.

308

309 *22154, 23: Please add a citation for this “old theory” of NAT PSC formation*

310

311 Added Koop et al. (1995) as a citation for this “old theory”.

312

313 *22154, 25: In my opinion the temperatures are never below T_{ice} .*

314

315 We changed “below T_{ice} ” to “near T_{ice} ”.

316

317 *22154, 25-28: The first sentence is maybe okay, but I don't know if this is really a proof for*
318 *the accuracy of the ERA Interim temperatures. I would say maybe a hint. But you have to*
319 *delete in any case the second sentence. It is presumptuous to claim that the ERA Interim*
320 *temperatures have an uncertainty of 1 K, because your model fits better with 1 K lower*
321 *temperatures.*

322

323 Your comment is right. We have deleted the second sentence.

324

325 *22156, 3-7: If it not possible to simulate the denitrification with ATLAS on your trajectories,*
326 *why do you use ATLAS then for this study? Or why do you show then comparisons of HNO3*
327 *and also of O3 between the model and the measurement? That make no sense in my opinion.*

328

329 We agree. We deleted panels and discussion related to O3 and HNO3.

330

331 *22156, 22-23: Cl2 can't be photolyzed to ClO_x because Cl2 is part of ClO_x.*

332

333 Cl2 is photolyzed to Cl, and then form ClO, which is a part of ClOx. We rephrased in the text.
334 We mistook the legend of ClOx in panels (f) (new panels (e)) of Figures 8 to 14. We changed
335 the species shown in panels in Figures 8 to 14.

336

337 *22156, 27: I don't see a chemical ozone depletion neither in ATLAS nor in the measurement.*
338 *ClO is the product of O3+Cl -> ClO, Cl is the reason for O3 depletion, not ClO.*

339

340 You are right. There is very small O3 depletion modelled by ATLAS at around day 2.8 and
341 3.5, when small solar illumination was available, which was shown by orange dots on the top
342 of panel (i) in Figure 9. However, O3 depletion is not the main issue of the focus of this paper,
343 we deleted description related to O3 from the draft.

344

345 *22157, 11: Cl₂ is photolyzed to Cl, not to ClO.*

346

347 See reply to comment 22156, 22-23. The text was rephrased.

348

349 *22157, 12: I would say “slightly” is the wrong word for this depletion.*

350

351 All the discussion on HNO₃ is removed from the manuscript.

352

353 *22157, 13-15: Again I don’t see really an ozone depletion.*

354

355 We deleted description related to O₃ from the draft.

356

357 *22157, 28-22158, 2: Why do you have such a decrease in HCl and ClNO₃ in the STS run (and*
358 *also in the STS-NAT run), although you simulate only a very small PSC surface area?*

359

360 Surface area density does not directly translate into reaction rates. The reaction rate is also
361 dependent on the amount of ClONO₂ available and temperature. E.g., in Figures 8-10, the
362 model just runs out of ClONO₂. In this case, it does not matter that the surface area densities
363 are much larger.

364

365 *22158, 12: Is the result of the -1 K model run really better than the standard model run? In*
366 *the first simulation you have in average smaller values as measured, in the second simulation*
367 *you have in average higher values as measured. In my opinion both runs fit well with MLS*
368 *regarding HCl. But in both runs the simulated PSCs don’t match the observations and also*
369 *the denitrification is not really better in the -1 K run.*

370

371 Since there is not enough difference between three PSC model runs, we only show
372 “STS+NAT” run results in the draft. We believe that temperature difference of 1 K is
373 important for the simulation result.

374

375 *22158, 13-15: That is surely a correct suggestion, but not really a new result, or?*

376

377 We modified the text to refer earlier result by Carslaw et al. (1994).

378

379 *22158, 24-26: You have also to delete this sentence. There is really no proof in your study for*
380 *any uncertainties in ECMWF temperatures.*

381

382 The sentence was deleted as suggested.

383

384 *22159, 1: Surely the HCl results are better in this case with the -1 K model run, but quite*
385 *well?*

386

387 We want to keep as it is.

388

389 *22160, 13-15: This is also my opinion. What is the reason that you show the results of all*
390 *these scenario runs in this publication?*

391

392 We modified to show only “STS+NAT” result in the draft.

393

394 *22161, 20-23: If you write as on page 22159, 18-19, that your study “suggest the possibility*
395 *of heterogeneous nucleation of NAT on solid particles” I can live with it, but here you*
396 *mention again the meteoritic dust, although you write on page 22159, line 16-17 that this*
397 *case is unlikely (Biermann et al., 2006).*

398

399 We added the description on Biermann et al. (1996) here as well as on page 22159.

400

401 *22162, 11: Please write here CIO instead CIO_x.*

402

403 Changed as suggested.

404

405 *22162, 24-27: It is not true that the temperature explain most discrepancies between model*
406 *and observation. Please correct this sentence. Also in the -1 K run you don't match PSC*
407 *periods from CALIOP or the HNO3 MLS measurements.*

408

409 We rephrased here to more focus on modeled and measured HCl discrepancies. The PSC
410 field is created by taking the closest CALIOP measurement, and sometimes not represent the
411 fine structure of actual PSC field. (Please see our reply to other referee (#1) major comment
412 3.)

413

414

415 < FIGURES >:

416

417 *Fig.1: last sentence: “.. and the Type II (ice) frost point temperature ..”*

418

419 Changed as suggested.

420

421 *Fig.3: Can you please also plot the colour bar which indicates the different PSC types in the*
422 *panels b and c. This is in my opinion important because the colour code is different to panel a*
423 *(otherwise it is confusing). If it possible it would also be great to write the longitudes and*

424 *latitudes to the horizontal axis of panel b and c (in the same way as in panel a). In panel c you*
425 *have two blue lines, maybe you can choose light blue in one case instead of blue.*

426

427 Color bar which indicates the different PSC types were added in panels (b). The longitudes
428 and latitudes was not added to panels (b) and (c), because it is not a very useful information
429 for the reader. The color of PSC saturation temperature was modified as suggested.

430

431 *Fig.4. to 14: Same as in Fig. 3: Please add a colour bar with the PSC types and the latitudes*
432 *and longitudes of the trajectories.*

433

434 Changed as suggested. The latitudes and longitudes of the trajectories were not added.

435

436 *Fig.5: a) Can you please add in the caption at least the information about time and altitude*
437 *and/or pressure for the trajectories cases? b) Why is the sequence #1, #4,#3 and not #1,#3,#4*
438 *c) Why do you show #3 and #4 both, this trajectories have more or less the same conditions*
439 *due to the very similar starting point? d) Again information about the latitudes and longitudes*
440 *of the trajectories and a colour bar would be great.*

441

442 The time and altitude information was added to the caption of Fig. 5. The sequence was re-
443 ordered. The case #03 was removed. The color bar was added. Latitudes and longitudes of
444 the trajectories were not added.

445

446 *Figs.6. and 7: Same as in Fig.5: More information would be great and the sequence is*
447 *strange.*

448

449 Cases were re-ordered.

450

451 *Fig.8: a) Temperature of trajectory case #3 is only displayed in Fig.5 not in Figs.5-7. b) It's*
452 *difficult to read the titles and the units in the panels. c) In general the panels are very small*
453 *(maybe this is better in the final paper?). For example the line of the grey curve of the STS*
454 *run is extremely difficult to see. d) In Fig. 8h I see also a dashed blue line. What is the*
455 *meaning of this line or is this a mistake?*

456

457 Since we deleted old panels (c) Rates, (h) HNO₃, and (i) O₃, the new figures 8-14 consists of
458 six panels. We hope this will improve the readability of each line. The HNO₃ panel (h) was
459 deleted.

460

461 *Fig.9: There is again this dashed blue line in panel h.*

462

463 The old HNO₃ panel (h) was deleted.

464

465 *Fig.12: a) There are again dashed blue lines in panel h. b) The comparison of measurements*
466 *and model is in the -1 K run not very good. The surface area density and the HNO₃ don't*
467 *match the observations. Why do you select this trajectory? Is this really the best comparison*
468 *you have (you write you analysed more than 30 trajectories).*

469

470 The old HNO₃ panel (h) was deleted.

471

472

473

474

475

Version ~~5.2a~~4.7f

476

~~31~~ ~~15~~ ~~January~~ ~~July~~ 201~~6~~5 (~~Sun~~Wed)

477

478

479 **Polar Stratospheric Cloud evolution and chlorine activation**
480 **measured by CALIPSO and MLS, and modelled by ATLAS**

481

482 **H. Nakajima^{1,2,*}, I. Wohltmann², T. Wegner³, M. Takeda⁴, M. C. Pitts³, L. R. Poole⁵, R.**
483 **Lehmann², M. L. Santee⁶, and M. Rex²**

484

485 [1] National Institute for Environmental Studies, Tsukuba, 305-8506, Japan

486 [2] Alfred Wegener Institute for Polar and Marine Research, Potsdam, 14473, Germany

487 [3] NASA Langley Research Center, Hampton, Virginia, 23681, USA

488 [4] Graduate School of Tohoku University, Sendai, 980-8579, Japan

489 [5] Science Systems and Applications, Incorporated, Hampton, Virginia 23666, USA

490 [6] Jet Propulsion Laboratory, California Institute of Technology, Pasadena, California 91109,
491 USA

492 [*] Now at Council for Science, Technology and Innovation, Cabinet Office, Government of
493 Japan, Tokyo, 100-8914, Japan

494

495

496 Corresponding author: H. Nakajima (nakajima@nies.go.jp)

497

498

499 **Abstract**

500 We examined observations of polar stratospheric clouds (PSCs) by CALIPSO and of HCl,
501 ~~and ClO and HNO₃~~ by MLS along air mass trajectories to investigate the dependence of the
502 inferred PSC composition on the temperature history of the air parcels, and the dependence of
503 the level of chlorine activation on PSC composition. Several case studies based on individual
504 trajectories from the Arctic winter 2009/2010 were conducted, with the trajectories chosen
505 such that the first processing of the air mass by PSCs in this winter occurred on the trajectory.
506 Transitions of PSC composition classes were observed to be highly dependent on the
507 temperature history. In cases of a gradual temperature decrease, nitric acid trihydrate (NAT)
508 and super-cooled ternary solution (STS) mixture clouds were observed. In cases of rapid
509 temperature decrease, STS clouds were first observed, followed by NAT/STS mixture clouds.
510 When temperatures dropped below the frost point, ice clouds formed, and then transformed
511 into NAT/STS mixture clouds when temperature increased above the frost point. The
512 threshold temperature for rapid chlorine activation on PSCs is approximately 4 K below the
513 NAT existence temperature, T_{NAT} . Furthermore, simulations of the ATLAS chemistry and
514 transport box model along the trajectories were used to corroborate the measurements and
515 show good agreement with the observations. Rapid chlorine activation was observed when an
516 airmass encountered PSCs. ~~The observed and modelled dependence of the rate of chlorine~~
517 ~~activation on the PSC composition class was small.~~ Usually, chlorine activation was limited
518 by the amount of available ClONO₂. Where ClONO₂ was not the limiting factor, a large
519 dependence on temperature was evident.

520

521

522 1. Introduction

523 Soon after the discovery of the Antarctic “ozone hole” (Farman et al., 1985), it was
524 established that heterogeneous reactions on polar stratospheric clouds (PSCs) play an
525 important role in ozone destruction (Solomon et al., 1986; [Portmann et al., 1996](#); [Solomon et](#)
526 [al., 2015](#)). They are the first step in the conversion of chlorine reservoir species (ClONO₂ and
527 HCl) to highly reactive radical species (Cl, ClO) which drive catalytic cycles that destroy
528 ozone (e.g., Molina and Molina, 1987).

559 PSC particles may be solid, consisting of ice (cf. the historical overview by Peter and Grooß,
560 | 2012) or nitric acid trihydrate (NAT: $\text{HNO}_3 \cdot 3\text{H}_2\text{O}$) (Crutzen and Arnold, 1986; Voigt et al.,
561 2000). Alternatively, they may also be liquid H_2O - H_2SO_4 - HNO_3 droplets (super-cooled
562 ternary solution = STS) (Carslaw et al., 1994). Liquid and solid particles can coexist over a
563 wide range of conditions (Koop et al., 1997; Pitts et al., 2009).

564 The mechanisms by which NAT particles are formed have provoked some controversy (for a
565 review, see Peter and Grooß, 2012). Laboratory measurements have shown that
566 homogeneous nucleation of NAT in H_2O - H_2SO_4 - HNO_3 solutions is kinetically limited, and
567 thus cannot be expected immediately after the existence temperature of NAT ($T_{\text{NAT}} \approx 195$ K
568 in the lower stratosphere) is reached (Koop et al., 1995). Another proposed NAT formation
569 mechanism is heterogeneous nucleation on ice particles (Koop et al., 1995), which requires
570 temperatures below the ice frost point ($T_{\text{ice}} \approx 188$ K in the lower stratosphere). However,
571 NAT PSCs have been observed by both in-situ aircraft and satellite measurements in air
572 masses that had not been exposed to temperatures below T_{ice} (e.g., Pagan et al., 2004; Larsen
573 et al., 2004; Voigt et al., 2005; Pitts et al., 2011). Therefore, heterogeneous nucleation of
574 NAT on meteoritic dust has been considered as an alternative “fast track” to NAT formation
575 | at temperatures above the frost point (Voigt et al., 2005; Hoyle et al., 2013); contrary to
576 Biermann et al. (1996) who showed in laboratory experiments that heterogeneous nucleation
577 rates on micrometeorites are too low to enhance freezing of PSCs above the frost point.

578 The uptake of chemical species, e.g. HCl, by PSC particles and the subsequent
579 heterogeneous reaction rates depend on PSC particle composition and surface area density
580 (and hence strongly on temperature). Chlorine reservoir species are converted into active
581 chlorine species by heterogeneous reactions on the surface of PSCs through:



585 Although chlorine activation on PSCs is an essential step towards ozone depletion, under
586 certain conditions the ozone loss may be rather insensitive to the rate constants of those
587 heterogeneous reactions and thus to the composition of PSCs present (e.g., Drdla and
588 Schoeberl, 2003; Wohltmann et al., 2013). For instance, this sensitivity is expected to be

589 small if the PSCs exist long enough so that one reaction partner of a heterogeneous reaction
590 becomes almost completely depleted. It is also small if one of the reaction partners has
591 already been depleted and its re-generation by gas-phase chemistry is slower than the
592 heterogeneous reactions.

593 According to the above-mentioned findings, the following questions are relevant for
594 understanding ozone depletion:

- 595 1) Which PSC compositions form under which conditions?
596 2) How sensitively do chlorine activation ~~and, consequently, ozone depletion~~ depend on
597 PSC composition?

598 In order to investigate Question 1, we used PSC observations by the CALIOP (Cloud-
599 Aerosol Lidar with Orthogonal Polarization) instrument on the CALIPSO (Cloud-Aerosol
600 Lidar and Infrared Pathfinder Satellite Observations) satellite in the Arctic winter 2009/2010
601 and temperature data from ECMWF (European Centre for Medium-Range Weather Forecasts)
602 analyses on backward trajectories initiated at the locations of the PSC observations. All three
603 PSC compositions mentioned above (STS, NAT, ice) were observed. These analyses show
604 that the PSC particle composition depends not only on the temperature at the time of the
605 observation, but also on the temperature history of the air parcel. This conclusion is in
606 agreement with the findings of Lambert et al. (2012), who used a similar approach with
607 CALIOP PSC composition and Aura Microwave Limb Sounder (MLS) HNO₃ data to analyse
608 PSC and HNO₃ evolution.

609 In order to study Question 2, we investigated the temporal evolution of HCl in the vicinity of
610 observed PSCs. For this, we calculated backward and forward trajectories from the positions
611 of the CALIOP PSC observations and considered Aura MLS HCl measurements within a
612 certain distance ("Match radius") from those trajectories. The signature of chlorine activation
613 seen in the HCl data was compared to simulations from the Lagrangian chemistry-transport
614 model ATLAS (Wohltmann et al., 2010). ~~Additional runs of this model were carried out to~~
615 ~~estimate the sensitivity of chemical ozone depletion to different PSC compositions.~~

616 We concentrated on the time period of the first occurrence of PSCs during the winter (mid-
617 December 2009 – beginning of January 2010). This choice allowed us to rule out the prior
618 existence of PSCs and associated repartitioning of chlorine-containing species by

619 heterogeneous reactions. This winter was one of the coldest winters in the Arctic during the
620 CALIPSO operation period when ice PSC was observed by the CALIOP measurements.

621

622

623 2. Data

624 2.1 CALIPSO/CALIOP PSC Data

625 CALIPSO, a component of the A-train satellite constellation (Winker et al., 2007, 2009),
626 was launched in April 2006 into a 98.2° inclination orbit that provides extensive daily
627 measurement coverage over the polar regions of both hemispheres up to 82° in latitude.
628 CALIOP, the primary instrument on CALIPSO, measures backscatter at wavelengths of 1064
629 and 532 nm, with the 532-nm signal separated into orthogonal polarization components
630 parallel and perpendicular to the polarization plane of the outgoing laser beam.

631 Pitts et al. (2007, 2009, 2011) developed a procedure for detecting PSCs using the CALIOP
632 532-nm scattering ratio (R_{532} , the ratio of total to molecular backscatter) and the 532-nm
633 perpendicular backscatter coefficient. They further developed an algorithm to classify PSCs
634 by composition based on the measured CALIOP aerosol depolarization ratio (δ_{aerosol} , the ratio
635 of perpendicular to parallel components of aerosol backscatter) and inverse scattering ratio
636 ($1/R_{532}$). Pitts et al. (2009) defined four composition classes of PSCs, i.e., STS, ice, Mix 1,
637 and Mix 2. Mix 1 and Mix 2 denote mixtures of liquid droplets with NAT particles in lower
638 or higher number densities/volumes, respectively. Pitts et al. (2011) added two additional
639 sub-classes of PSCs, i.e., Mix 2 enhanced, and wave ice PSCs.

640 In this study, we used three categories of PSCs from CALIOP data: STS, Mix (which
641 includes Mix 1, Mix 2, and Mix 2 enhanced), and ice (which includes ice and wave ice) PSCs.

642 In order to assign PSC composition along the trajectories, we selected the composition of the
643 CALIOP measurement location that was closest to each trajectory point on the same day. For
644 each trajectory point, the horizontally closest CALIOP measurement profile was first
645 determined and then the PSC classification closest in potential temperature to the trajectory
646 point was taken from this measurement profile. An analogous method was used to produce
647 the maps in Figure 2.

648 Due to the sampling pattern of CALIOP, there is some intrinsic and unavoidable uncertainty
649 in the PSC characterizations at any given location, which is typically some distance away
650 from the point being measured by CALIOP. The approach we have used relies on the
651 assumption that PSCs are sufficiently homogeneous on a spatial scale that corresponds to the
652 average distance to the next measurement, which is about 100-200 km, and a time difference
653 within 24 hours.

654

655

656 2.2 MLS Data

657 This study also uses data from the Microwave Limb Sounder (MLS) instrument on the Aura
658 satellite (Waters et al., 2006). The Earth Observing System (EOS) Aura satellite was
659 launched on 15 July 2004 and has been in operation since August 2004 making measurements
660 between 82° N and 82° S. MLS measures millimeter- and submillimeter-wave thermal
661 emission from the limb of Earth's atmosphere. We use MLS version 3.3 HCl, ClO, ~~HNO₃~~,
662 and ~~HO₃~~ data (Livesey et al. 2006, 2013). Vertical resolution of MLS data is ~3 km in the
663 lower stratosphere at 100-10 hPa. A discussion of the quality of MLS measurements can be
664 found in Livesey et al. (2013). Error bars in the figures that follow indicate the 1 σ precision
665 of the measurements.

666

667 3. Analysis Method

668 3.1 PSC evolution in the northern winter 2009/2010

669 In the Arctic winter 2009/2010, PSCs started to appear in mid-December 2009 at around 23
670 km when the minimum temperature dropped below the nitric acid trihydrate saturation
671 temperature T_{NAT} (Pitts et al., 2011). Figure 1 shows the temporal variation of the minimum
672 temperature (T_{MIN}) between 50 and 90°N at the 30 hPa pressure level. ~~The thick black line is~~
673 ~~the mean over the winters 1978/79 to 2013/14, while the thin black lines are minimum and~~
674 ~~maximum temperatures. The thick red line shows the variation of the daily minimum~~
675 ~~temperature in the 2009/2010 Arctic winter.~~ The two green lines show the NAT and ice PSC

676 threshold temperatures (T_{NAT} and T_{ice} , respectively) calculated by assuming 6 ppbv of HNO_3
677 and 4.5 ppmv of H_2O . T_{MIN} dropped below T_{NAT} at the middle of December and below T_{ice} at
678 the end of December 2009 and again in mid-January. A sudden stratospheric warming
679 terminated the period with temperatures below T_{NAT} at the end of January 2010 (Dörnbrack et
680 al., 2012).

681 The PSC observations of CALIOP are consistent with the temperature history in this winter.
682 Figure 2a shows an example of the PSC field on the 550 K potential temperature surface for
683 21 December 2009 with CALIOP observation points, when substantial PSC coverage was
684 first observed by CALIOP at this altitude (~23 km) in this Arctic winter. Global PSC field
685 was created by selecting the closest CALIOP PSC measurement on the same day. Note that
686 the CALIOP PSC products are only produced for nighttime orbit segments due to higher
687 background lighting conditions during daytime. On 21 December 2009, the day/night
688 transition occurs near 72°N . Also note that the area north of 82°N is shadowed by grey color,
689 because there is no CALIPSO orbital coverage there. Similarly, Figure 2b shows an example
690 of the PSC field at 550 K for 1 January 2010, when the maximum extent of PSCs was
691 observed at this altitude. PSC fields were created in this way for each day during the
692 2009/2010 Arctic winter.

693

694 3.2 Selection of trajectories for the case studies

695 As mentioned in Section 1, backward and forward trajectories from the positions of
696 CALIOP PSC observations were calculated, in order to investigate the chemical effects of
697 these PSCs by analysing chemical model runs and trace gas observations along these
698 trajectories. In order to exclude any chemical effect of earlier PSCs in the analysed air masses,
699 we concentrate on the time period of early winter (between 19 December 2009 and 3 January
700 2010).

701 As a first step, several cases of CALIOP observations of PSCs of a clearly defined
702 composition class were selected. The selected cases encompass a range of different
703 conditions with respect to temperature and PSC classification. Two examples are presented in
704 Figures 3 and 4. In each case, a location in the center of such a PSC was selected. It was
705 marked by a cross and a label in Figure 3a (“n1”: mix 1 PSC), and Figure 4a (“e4”: mix 2

706 enhanced PSC). In order to show the temporal evolution of temperature and HCl in the
707 analysed airmass, 5-day backward and 5-day forward trajectories, starting at the marked
708 position, were calculated. The corresponding trajectory model is taken from the ATLAS
709 chemistry and transport box model (Wohltmann et al., 2010). Model runs are driven by
710 meteorological data from the ECMWF ERA Interim reanalysis (Dee et al., 2011), with time
711 resolution of 6h and horizontal resolution of 2 times 2 degrees. The vertical coordinate is
712 potential temperature and vertical motion is driven by total diabatic heating rates from ERA
713 Interim.

714 Figures 3b and 4b show MLS measurements of HCl along the path of the trajectories as a
715 function of time (green dots with error bars). All HCl measurements that were closer than
716 200 km to the position of the trajectory at a given point in time are plotted. PSC occurrence is
717 color coded in the background. Green shaded areas correspond to STS clouds, red shaded
718 areas to NAT/STS mixture clouds, and blue shaded areas correspond to ice clouds. Grey
719 areas correspond to sections of the trajectory north of 82°N, where no measurements from
720 CALIOP or MLS are available. Nevertheless, we can find some matched MLS points within
721 the grey area in Figure 3b. This is because MLS observations were selected within a match
722 radius of 200 km. Figures 3b and 4b show that HCl values were around 2 ppbv on the
723 backward trajectories and that either no PSCs were measured by CALIOP or no
724 measurements from CALIOP were available on the backward trajectory. HCl started to
725 decrease near $t=0$, a time at which PSCs were present according to our choice of the trajectory
726 starting points. Figures 3c and 4c show the temperature along the trajectories, with the PSC
727 occurrence as in Figures 3b and 4b. The thin black lines correspond to T_{NAT} and $T_{\text{NAT}} - 3$ K,
728 the thin blue line corresponds to T_{ice} . The threshold temperature for the formation of NAT
729 clouds (T_{NAT}) is based on the equations of Hanson and Mauersberger (1988). For the forward
730 part of the trajectory, HNO_3 and H_2O from the box model runs (cf. Section 4) were used for
731 the calculation of T_{NAT} . For the backward part of the trajectory, HNO_3 and H_2O values were
732 fixed at the starting values of the box model run. The threshold temperature for the formation
733 of ice (T_{ice}) was calculated in the same manner from the equations of Marti and Mauersberger
734 (1993). In the cases shown in Figures 3 and 4, the temperature does not drop below $T_{\text{NAT}} - 3$
735 K on the backward trajectory (before the occurrence of selected PSC). It can be seen that
736 when temperature decreased, PSCs started to form along the path of the forward trajectory.

737 In order to analyse the temporal evolution of chemical species after the encounter of PSCs,
738 ATLAS box model runs, which will be explained in the following Section in detail, will be
739 performed on several trajectory cases. It is desirable to start these model runs from initial
740 concentrations that have not been influenced by any earlier PSC occurrence in the airmass of
741 interest. However, if these model runs started at the locations selected in the center of a PSC
742 (as those marked in Figures 3a and 4a), then a part of the backward trajectory would lie
743 within the selected PSC. Consequently, some chlorine activation might occur already before
744 the beginning of the forward trajectory. In order to avoid this effect, the forward trajectories
745 for the runs of the ATLAS box model are started before the encounter of the selected PSC.
746 For this, a new starting point (corresponding to a new starting time $t=0$) of the trajectory
747 calculations was selected on the original backward trajectory such that it fulfills the following
748 conditions: (1) There is no PSC in the CALIOP data near the backward trajectory before the
749 new starting time. (2) The temperature at and before the new starting time does not drop
750 below $T_{\text{NAT}} - 3$ K. The assumption behind this is that a supersaturation of a factor of about 10
751 (3 K supercooling) is needed for the formation of NAT clouds and that STS clouds only take
752 up measureable quantities of HNO_3 below $T_{\text{NAT}} - 3$ K (Dye et al., 1992; Pitts et al., 2007). (3)
753 The matched MLS HCl values at and before the new starting time were above ~ 2 ppbv, which
754 proves that the airmass has not been processed by PSCs before the new $t=0$. In such a way,
755 we selected ~ 30 trajectory cases in early winter between 19 December 2009 and 3 January
756 2010 for several PSC classes. Then we selected 11 trajectories for case studies, which cover
757 several different PSC composition classification and different temperature histories. The new
758 trajectory starting points are (summarised in Table 1.) ~~for case studies.~~ Starting from these
759 points, new 5-days forward and 5-days backward trajectories were calculated. ATLAS box
760 model was run on these 5-days forward trajectories, which passed through the center part of
761 the selected PSCs.

762

763

764 4. ATLAS model

765 4.1 Model description

796 The box model runs, simulating the temporal evolution of chemical species along the
797 trajectories described in Section 3.2, use the chemistry box model of the ATLAS
798 (Wohlmann et al., 2010). Updates to the chemistry model and PSC model are described in
799 Wohlmann et al. (2013). The model includes a gas phase stratospheric chemistry module and
800 heterogeneous chemistry on PSCs. It comprises 47 active species and more than 180
801 reactions. Absorption cross sections and rate coefficients are taken from recent JPL
802 recommendations (Sander et al., 2011). The chemical model runs are driven by
803 meteorological data from the ECMWF ERA Interim reanalysis (Dee et al., 2011).

804 The treatment of conditions where both NAT and STS PSCs are allowed to form in parallel,
805 the model has changed compared to Wohlmann et al. (2013) to allow for more realistic
806 behavior. In Wohlmann et al. (2013), only liquid clouds could form between T_{NAT} and the
807 temperature corresponding to the assumed supersaturation for HNO_3 over NAT. At
808 temperatures below that of the assumed supersaturation, NAT clouds would form first,
809 usually consuming all available HNO_3 and impeding the formation of ternary liquid clouds
810 (by chance, the temperature where binary liquid aerosols begin to take up HNO_3 in
811 measurable quantities is about the same as the temperature where NAT clouds begin to form
812 in the model). Since NAT/STS mixtures are commonly observed (e.g. Pitts et al., 2011), we
813 implemented a simple algorithm that allows for mixed clouds: If the given supersaturation of
814 HNO_3 over NAT is exceeded, only a predefined fraction of the amount of HNO_3 that has to be
815 removed from the gas phase to reach the supersaturation again is allowed to go into NAT
816 clouds. The remaining fraction is available for the formation of STS clouds. The fraction is
817 set to 0.2 for our model runs.

818

819 **4.2 Sensitivity runs**

820 ~~Three sensitivity runs with different assumptions on PSCs are performed for each trajectory.~~
821 ~~In the “STS+NAT” run, PSC information from CALIPSO is ignored and the box model forms~~
822 ~~PSCs according to temperature and available condensable HNO_3 and H_2O , in the same way as~~
823 ~~described in Section 4.1.~~

824 In the ATLAS model run ~~this run~~, the NAT particle number density is set to 0.1 cm^{-3} , the ice
825 particle number density is set to 0.01 cm^{-3} , and the STS droplet number density is set to 10

書式変

826 cm^{-3} . A supersaturation of HNO_3 over NAT of 10 (corresponding to about 3 K supercooling)
827 is required for NAT particle formation. A detailed discussion of the rationale behind these
828 choices can be found in Wohltmann et al. (2013). For ice particles formation, a
829 supersaturation of 0.35 is assumed based on MLS satellite measurements of H_2O and
830 ECMWF temperatures. Reaction rates for NAT particles are based on scheme 1 in Carslaw et
831 al. (1997) and reaction rates for liquid particles are based on Hanson and Ravishankara (1994).

832 ~~The “STS” run is identical to the “STS+NAT” run, except that no NAT clouds are allowed~~
833 ~~to form.~~

834 ~~The “CALIPSO constrained” run uses the information from the CALIPSO satellite to~~
835 ~~constrain the formation of PSC within the model. Five different cases are considered:~~

836 ~~1. If CALIOP measures no PSCs, no clouds are formed in the box model runs.~~

837 ~~2. If CALIOP detects only STS, then STS is allowed to form according to temperature and~~
838 ~~species mixing ratios in the box model, as explained above. Note that in the “STS+NAT” and~~
839 ~~“STS” runs, STS may form outside of the area where CALIOP detects STS clouds, if the~~
840 ~~temperature conditions are appropriate. However, in the “CALIPSO constrained” run, the~~
841 ~~model will not form STS outside of the area where CALIOP detects STS. In addition, if~~
842 ~~CALIOP detects STS in a region where ECMWF temperatures are too warm for STS~~
843 ~~existence, the model will only produce binary liquid aerosol.~~

844 ~~3. If CALIOP detects mixed clouds, both STS and NAT clouds are simulated in the box~~
845 ~~model. STS clouds are simulated in the same way as above. NAT clouds are formed with a~~
846 ~~predefined number density of 10^{-3}-cm^{-3} and a predefined radius of $2\text{-}\mu\text{m}$.~~

847 ~~4. If CALIOP detects ice clouds, ice clouds are formed with a predefined number density of~~
848 ~~1-cm^{-3} and a predefined radius of $5\text{-}\mu\text{m}$.~~

849 ~~5. There are no CALIOP measurements north of 82°N . In this region, the “CALIPSO~~
850 ~~constrained” run uses the same setting as the “STS+NAT” run.~~

851 ~~The NAT and ice cloud number densities used here were derived by comparing the 2-D~~
852 ~~histograms of CALIOP PSC observations (Figure 4 in Pitts et al., 2009) and theoretical~~
853 ~~calculation of NAT and ice PSC growth (Figures 5 and 6 in Pitts et al., 2009). Note that while~~

854 ~~these numbers are plausible under atmospheric conditions, particles in the real atmosphere~~
855 ~~may exist over a wide range of sizes and number densities (e.g., Wegner et al., 2012).~~

856

857 **4.23 Chemical initialization**

858 The model chemical initialization is performed in three steps. First, all of the species are
859 initialized from the mixing ratio fields of an existing global model run of ATLAS for the
860 winter 2009/2010 (the reference run in Wohltmann et al., 2013). For this, a short back
861 trajectory is calculated from the starting position of each trajectory back to the time of the last
862 model output of the global model run preceding the start date of the trajectory. The chemical
863 model is then run forward on this short trajectory with the initialization taken from the nearest
864 air parcel of the global model output.

865 In the second step, mixing ratio values for HCl, O₃ and H₂O are replaced by measurements
866 from MLS. MLS gas-phase HNO₃ observations are not used, in order to avoid problems
867 when some of the total available HNO₃ is in the condensed phase (the model needs total
868 HNO₃ and MLS measures gas phase HNO₃). The MLS values for HCl, O₃ and H₂O are
869 obtained by calculating a 5-day back trajectory from the starting point of each trajectory and
870 calculating an average over all MLS measurements close to the trajectory (with a match
871 radius of 200 km). In order to keep Cl_y (the sum of all inorganic species containing chlorine)
872 constant at the value specified by the global ATLAS runs, the difference between the MLS
873 HCl value and the HCl value of the global model run is added to (or subtracted from,
874 depending on sign) the mixing ratio of ClONO₂. Note that no chlorine activation has yet
875 taken place at the time when the model is initialized, and this correction does not produce
876 negative ClONO₂ values for any of the trajectories.

877 In some cases (trajectories #05, #08, and #10), modelled ClONO₂ is fully depleted before
878 HCl reaches the level indicated by the MLS measurements. In these cases, a third step is
879 applied to ensure that HCl and ClONO₂ are adjusted such that the amount of HCl loss in the
880 model matches the loss of HCl in the MLS data. In all of these cases, there is a significant
881 difference between the observed HCl mixing ratios before and after the PSC occurrence. The
882 magnitude of this observed drop in HCl is used as the initialization for ClONO₂, such that
883 ClONO₂ is nearly depleted at the end of the box model run. In order to keep Cl_y constant

884 again, the difference between the new ClONO_2 value (taken from the decrease in observed
885 HCl) and the old ClONO_2 value (after the first correction in the second step caused by MLS
886 HCl) is added to (or subtracted from) $\text{ClO}_x = \text{ClO} + 2\text{Cl}_2\text{O}_2$ in a way that preserves the
887 partitioning between ClO and Cl_2O_2 .

888

889

890 5. Results

891 5.1 Dependence of PSC classification on temperature history

892 In this section, we show the temporal change in PSC classification along ~~eight~~^{nine} selected
893 trajectories with different temperature histories.

894 Figures 5a-~~be~~ show cases in which the airmass cooled gradually over a period of days to
895 below $T_{\text{NAT}} - 3$ K. NAT/STS mixture PSCs started to appear when the airmass temperature
896 decreased below approximately $T_{\text{NAT}} - 4$ K in all cases shown. No ice PSCs and only a
897 negligible amount of STS PSCs were observed during the course of the trajectory. When
898 temperatures warmed above T_{NAT} , in trajectory case #1, the mixed PSCs mostly disappeared.
899 Since there was no region within the polar vortex with temperatures below the frost point
900 before these PSC events, the NAT/STS mixture PSC observed here was assumed to be
901 formed without any prior exposure to ice PSCs.

902 Figures 6a-c show cases in which the airmass temperature decreased rather rapidly due to
903 adiabatic cooling by orographic lift as it passed over Greenland. In these cases, STS formed
904 first as the temperature decreased below approximately $T_{\text{NAT}} - 4$ K, followed by a transition to
905 NAT/STS mixture PSCs as the temperature warmed to near T_{NAT} . When the temperature rose
906 above T_{NAT} , the PSCs disappeared.

907 Figures 7a-c show cases where the airmass temperature decreased rapidly to T_{ice} due to
908 adiabatic cooling by orographic lift as it passed over Greenland. In these cases, STS formed
909 first as the temperature decreased below approximately $T_{\text{NAT}} - 4$ K, followed by the formation
910 of ice as the temperature decreased to T_{ice} . As the temperature warms above T_{ice} , the ice PSC
911 is transformed into a NAT/STS mixture PSC, as suggested by an old theory of NAT PSC
912 formation (Koop et al., 1995). ~~With the exception of the #10 case, †~~The CALIOP ice PSC

943 observations coincide quite well with the trajectory segments ~~when with~~ air mass temperatures
944 ~~cooled near below~~ T_{ice} . This proves the accuracy of ECMWF ERA Interim reanalysis
945 temperature data to some extent even in a mesoscale scenario such as mountain-induced
946 adiabatic cooling event. ~~However, as will be discussed later, our model runs suggest that the~~
947 ~~uncertainty in ECMWF temperature is about 1 K.~~

948

949 5.2 Comparison of MLS measurements with the ATLAS model

950 In this section, we show the temporal changes of several parameters modelled by ATLAS
951 and compare these with Aura/MLS measurements.

952 Figures 8a-f show the trajectory case #03 that started at 07:58:21 UT on 23 December 2009.
953 It is not known if PSCs existed between 8 and 49 hours after the starting time of the forward
954 trajectory because the trajectory went into the polar region above 82°N latitude where there
955 are no CALIOP measurements. At hour 49, the air mass encountered STS and then NAT/STS
956 mixture PSCs as the temperature cooled below approximately $T_{NAT} - 4$ K as shown in Fig. ~~ure~~
957 8a. The surface area density ~~ies~~ of the PSCs calculated by ATLAS ~~for the three different~~
958 ~~sensitivity runs, i.e. the STS+NAT run, STS run, and “CALIPSO constrained run” are is~~
959 shown in Fig. ~~ure~~ 8b. ATLAS indicated a small increase in surface area density between days
960 1 and 2 when the temperature decreased approximately 4 K below T_{NAT} , where CALIOP was
961 not able to measure in that period due to the sampling limitation stated above. ~~Similarly, the~~
962 ~~calculated heterogeneous reaction rate of ClONO₂ + HCl on the PSC particles is shown in~~
963 ~~Figure 8c. Note that the reaction rate decreased more rapidly than the surface area of the~~
964 ~~PSCs. This is due to the total loss of ClONO₂ as will be discussed later in detail.~~ Figure 8c
965 shows the calculated and measured amount of HCl by ATLAS and by Aura/MLS,
966 respectively. MLS observations were matched to the trajectory with a match radius of 200
967 km, as was explained in Sect. ~~ion~~ 3.2. When the temperature decreased to about $T_{NAT} - 3$ K,
968 the calculated HCl started to decrease in all three model runs. Similarly, ClONO₂ started to
969 decrease and was fully depleted between days 2 and 3 as is shown in Fig. ~~ure~~ 8d. After this
970 point, HCl could not decrease anymore because the reaction partner (ClONO₂) was already
971 fully depleted. The measured and calculated HCl values agree quite well within the error bars
972 of MLS measurements as expected. The depleted chlorine was converted into Cl₂ or ClO_x as

書式変

973 is shown in Figure 8ef. Because little sunlight was present along the trajectory, only a small
974 amount of ClO_x exists in the form of ClO as is shown in Figure 8fg after day 4. ~~Figure 8h~~
975 ~~shows the calculated and measured amount of HNO₃ by ATLAS and by Aura/MLS,~~
976 ~~respectively. In the three different ATLAS model runs, different HNO₃ values were~~
977 ~~calculated. However, MLS HNO₃ values were much smaller than the modelled values in all~~
978 ~~three model runs after day 3. Since the denitrification module of the global ATLAS model is~~
979 ~~designed to work correctly only on larger spatial and time scales, it cannot reproduce the~~
980 ~~denitrification for a single trajectory correctly. Modelling HNO₃ correctly by ATLAS along~~
981 ~~individual trajectories is beyond the scope of this paper. Figure 8i shows the calculated and~~
982 ~~measured amount of O₃ by ATLAS and by Aura/MLS, respectively. Since there was not~~
983 ~~sufficient ClO available for catalytic ozone destruction due to the lack of solar illumination,~~
984 ~~both calculated and measured O₃ did not indicate any ozone depletion in this case.~~

985 Figures 9a-f show the trajectory case #05 that started at 17:53:38 UT on 30 December 2009.
986 The trajectory encountered a region of CALIOP STS measurements after 10 hours as the
987 temperature decreased below approximately $T_{\text{NAT}} - 5$ K. Between days 1 and 5, NAT/STS
988 mixture PSCs were observed along the trajectory, as well as a very short period of ice PSCs
989 between days 1 and 2 when the temperature cooled to T_{ice} . Calculated PSC surface area
990 density increased rapidly when the airmass temperature decreased below around $T_{\text{NAT}} - 3$ K
991 between days 0 and 2 as is shown in Figure 9b. However, both HCl and ClONO₂ stopped
992 decreasing just a few hours after the airmass encountered the STS PSCs, because the ClONO₂
993 was fully depleted within this time as is shown in Figures 9c-d and 9e and 9f. The measured
994 and calculated HCl values agree quite well. The depleted reservoir chlorine was first
995 converted into Cl₂, then after exposure to sunlight (indicated by orange dots on the upper part
996 of Figures 9g-i), Cl₂ was photolyzed to Cl which forms ClO_x (Figures 9ef and 9fg). The
997 measured and calculated ClO values also agree quite well. ~~The temporal evolution of HNO₃~~
998 ~~is shown in Figure 9h. The measured HNO₃ between days 2 and 5 is slightly depleted,~~
999 ~~suggesting the possibility of mild denitrification. A small amount of ozone depletion was~~
1000 ~~modelled by ATLAS in this case when sufficient ClO was available as is shown in Figure 9i.~~

1001 Figures 10a-f show the trajectory case #08 that started at 16:59:14 UT on 31 December
1002 2009. After 3 hours, the airmass encountered STS PSCs as the temperature decreased below
1003 approximately $T_{\text{NAT}} - 5$ K. As the temperature further decreased to reach T_{ice} after 20 hours,

1004 | ice PSCs were observed by CALIOP as is shown in Figure 10a. When the temperature
1005 | increased above T_{ice} after 23 hours, NAT/STS mixture PSCs were observed. This case is
1006 | quite similar to the previous case. Calculated PSC surface area density rapidly increased
1007 | when the airmass cooled to around T_{ice} between days 0 and 2 as shown in Figure 10b.
1008 | However, both HCl and ClONO₂ stopped decreasing just a few hours after the airmass
1009 | encountered STS PSCs, because ClONO₂ was fully depleted within this time as shown in
1010 | Figures 10cd and 10de. Also in this case, the measured and calculated HCl values agree
1011 | quite well. The depleted reservoir chlorine was first converted into Cl₂, then with exposure to
1012 | sunlight (indicated by orange dots on the upper part of Figures 10cd-10fi), Cl₂ was
1013 | photolyzed to Cl which was then converted into form ClO as shown in Figure 10fg. The MLS
1014 | ~~HNO₃ values were slightly depleted between days 1 and 3, suggesting the possibility of a~~
1015 | ~~small degree of denitrification. In this case, slight ozone destruction was modelled by~~
1016 | ~~ATLAS when there was sufficient ClO available, as is shown in Figure 10i. However, the~~
1017 | ~~uncertainty in the measured ozone is too large to deduce a quantitative ozone loss amount.~~

1018

1019 | 5.3 Temperature sensitivity study for ATLAS model runs

1020

1021 | Figures 11a-f show the trajectory case #02 that started at 08:09:30 UT on 21 December
1022 | 2009. After 55 hours, the airmass encountered STS PSCs as the temperature decreased below
1023 | $T_{NAT} - 4$ K for a while. Shortly afterwards, a mixed type PSC was observed by CALIOP.
1024 | When temperature increased to around T_{NAT} at day 4, STS PSC was observed again before the
1025 | airmass exited the PSC area. In this case, the time period when the temperature was below
1026 | $T_{NAT} - 4$ K was relatively short as is shown in Figure 11a. As a result, the higher values of
1027 | PSC surface area calculated by ATLAS were limited to a short time period at around day 2 as
1028 | is shown in Figure 11b. As a result, the decrease of both HCl and ClONO₂ modelled by
1029 | ATLAS was small, and ClONO₂ was not totally depleted even after passage through the PSCs.
1030 | In addition, the ~~modelled HCl and ClONO₂ are very sensitive to different PSC scenarios that~~
1031 | ~~are assumed in this case. The STS+NAT model run produces the largest decrease in the~~
1032 | ~~chlorine reservoirs, while the CALIPSO-constrained model run produces the smallest~~

1033 ~~decrease in the chlorine reservoirs. Moreover, all three ATLAS model runs underestimate~~
1034 ~~the loss of HCl compared with observations as is shown in Figure 11cd.~~

1035 In order to study the sensitivity of the ATLAS model runs to the ECMWF ERA Interim
1036 reanalysis temperatures, we made additional ATLAS model runs by introducing a ± 1 K
1037 temperature bias. Figures 12a-f show the same trajectory as Figures 11a-f with red and blue
1038 lines added to show the sensitivity runs with the temperature changed by ± 1 K, respectively.
1039 The reference run (black line) ~~used no temperature biases. is the STS+NAT run.~~ As is shown
1040 in Figures 12b-and-12e, a temperature change of only 1 K greatly affects the PSC surface
1041 area density ~~and heterogeneous reaction rate of ClONO₂ + HCl.~~ As a result, the modelled
1042 depletion of HCl and ClONO₂ are also significantly affected as is shown in Figures 12cd and
1043 12de. In fact, the minus 1 K model run result agrees fairly well with the MLS HCl
1044 observations as shown in Figure 12cd. This result suggests the previous studies (e.g.,
1045 Carlsaw et al., 1994) that very accurate temperature data are required to correctly model the
1046 heterogeneous reactions on PSCs at temperatures near $T_{\text{NAT}} - 4$ K.

1047 Figures 13a-f show another example; trajectory case #09 which started at 18:35:15 UT on
1048 31 December 2009. After 18 hours, the air mass encountered NAT/STS mixture PSCs as the
1049 temperature decreased below approximately $T_{\text{NAT}} - 3$ K. In this case, the time period when
1050 the temperature was below $T_{\text{NAT}} - 3$ K was very short (less than 10 hours), as is shown in
1051 Figure 13a. Accordingly, the modelled increase of PSC surface area density ~~and~~
1052 ~~heterogeneous chlorine activation were~~ was very small as is shown in Figures 13b-and-13e.
1053 Consequently, the model did not produce substantial HCl or ClONO₂ depletion around day 1,
1054 as shown in Figures 13cd and 13de. However, MLS HCl measurements do indicate some
1055 depletion between days 2 and 4, as shown in Figure 13cd. ~~These results again suggest the~~
1056 ~~uncertainty of ECMWF temperature compared with the actual temperature.~~

1057 Figures 14a-f show the results of the temperature sensitivity study for case #09. As shown
1058 by Figures 14b-and-14e, perturbing the ECMWF temperature field by minus 1 K greatly
1059 increases the likelihood of PSCs around day 1. Consequently, the modelled HCl depletion for
1060 the minus 1 K case agrees with the MLS measurements quite well as shown in Figure 14cd.
1061 This result again illustrates the importance of accurate temperature data especially when the
1062 temperature is around $T_{\text{NAT}} - 4$ K, which is the approximate threshold temperature of
1063 NAT/STS mixture and STS PSC formation.

1064

1065

1066 6. Discussion

1067

1068 | In Section 5.1, we showed three typical temperature histories for PSC formation, i.e.,
1069 | gradual temperature decrease, rapid temperature decrease, and temperature decrease below
1070 | T_{ice} . Figures 5a-b show the formation of NAT/STS mixture PSCs for the case of gradual
1071 | temperature decrease in airmasses that have never experienced temperatures below T_{ice} .
1072 | These cases clearly show the existence of an ice-free nucleation mechanism of NAT, as was
1073 | previously suggested by Drdla et al. (2003), Larsen et al. (2004), Pagan et al. (2004), Voigt et
1074 | al. (2005), Pitts et al. (2011), and Hoyle et al. (2013). The homogeneous nucleation of NAT
1075 | in $H_2O-H_2SO_4-HNO_3$ solutions is kinetically strongly hampered and thus cannot be expected
1076 | (Koop et al., 1997). One of the possible mechanisms for NAT formation is heterogeneous
1077 | nucleation on solid particles such as meteoritic dust, as was postulated by Iraci et al. (1995),
1078 | although Biermann et al. (1996) suggested that heterogeneous nucleation rates on
1079 | micrometeorites are too low to enable freezing of NAT PSCs. Our results suggest the
1080 | possibility of heterogeneous nucleation of NAT on solid particles as is already pointed out by
1081 | Hoyle et al. (2013).

1082 | When the airmass temperature cooled rapidly due to adiabatic cooling by passage over
1083 | mountain ranges, STS PSCs first formed as the temperature decreased below approximately
1084 | $T_{NAT} - 4$ K as shown in Figures 6a-c. As the airmass temperature began to increase, a
1085 | transition to NAT/STS mixture PSCs was observed without the existence of ice, especially for
1086 | the case #06. Such a case was previously reported in PSC observations by backscatter sondes
1087 | in the Arctic by Larsen et al. (1997). This result also indicates the possibility of ice-free
1088 | formation of NAT.

1089 | Figures 7a-c show the cases when the airmass temperature decreased rapidly below T_{ice} due
1090 | to adiabatic cooling over mountain ranges. As the airmass temperature began to increase, a
1091 | transition to NAT/STS mixture PSCs was observed in all these cases. NAT/STS mixture
1092 | PSCs usually disappear when the temperature warms above T_{NAT} . These cases are consistent
1093 | with the ice-assisted nucleation mechanism of NAT suggested by Carslaw et al. (1995).

1094 In Section 5.2, comparisons of MLS HCl, ClO, ~~HNO₃~~, and O₃ measurements with ATLAS
1095 model simulation results were shown for the trajectory cases #03, #05, and #08. Figures 8a-f
1096 shows the gradual temperature decrease case #03, Figures 9a-f shows the rapid temperature
1097 decrease case #05, and Figure 10a-f shows the temperature decrease below T_{ice} case #08. In
1098 all three cases, measured and modelled HCl and ClO agree fairly well, ~~irrespective of the~~
1099 ~~three model scenarios, i.e., “STS+NAT”, “STS”, and “CALIPSO constrained”.~~ The
1100 ~~difference in modelled HCl and ClO among the three scenario runs was very small and it is~~
1101 ~~difficult to tell which scenario most closely fits the measurements.~~ In other words, if the
1102 ~~airmass cooled below approximately T_{NAT} - 4 K for a longer time and consequently there was~~
1103 ~~substantial chlorine activation on PSCs, the PSC classification has little impact on the details~~
1104 ~~of the chlorine activation.~~ The chlorine activation usually occurred very rapidly within a few
1105 hours. The amount of HCl loss was shown to be limited by the available ClONO₂ amount.
1106 After all the ClONO₂ has been converted into ClO_x, HCl cannot be further depleted as
1107 previously shown in a model study by Müller et al. (1994).

1108 In Section 5.3, similar comparison results were shown for the cases #02 and #09, when the
1109 airmass temperature was below approximately T_{NAT} - 4 K for only a short time period. In
1110 these trajectory cases, the depletion of HCl and activation of ClO was underestimated by the
1111 model in comparison to the MLS measurements, ~~for all three model scenarios, although the~~
1112 ~~“STS+NAT” and “CALIPSO constrained” runs were closer to the measurements than the~~
1113 ~~“STS” run.~~ In these cases, ClONO₂ was not totally depleted after passage through the PSCs.
1114 In cases where only a small amount of chlorine is activated, the amount of chlorine activation
1115 on PSCs is very dependent on ~~PSC classification and/or~~ airmass temperature. In fact,
1116 changing the ECMWF ERA Interim temperature field used as input to the ATLAS model by
1117 ±1 K has a large impact on the resulting magnitude of chlorine activation as shown in Figures
1118 12a-f and 14a-f. The large temperature sensitivity around T_{NAT} - 4 K can be attributed to
1119 the fact that both PSC surface area density and heterogeneous reaction probability (gamma
1120 value) increase quite rapidly around this temperature. Therefore, we conclude that quite
1121 accurate temperature knowledge is needed to correctly model the chlorine activation amount
1122 at around T_{NAT} - 4 K.

1123

1124

1125 7. Conclusions

1126

1127 We performed trajectory analyses to study the evolution of PSC composition and chlorine
1128 activation from the reservoir species of HCl and ClONO₂. We investigated which PSCs form
1129 according to measurements of CALIOP as a function of the temperature history along the
1130 trajectories. We studied 11 individual trajectories in the early Arctic winter 2009/2010. In
1131 cases of a gradual temperature decrease below approximately $T_{\text{NAT}} - 4$ K, NAT/STS mixture
1132 PSCs appeared first. In these cases, ice PSCs were not observed by CALIOP before the
1133 formation of the mixed clouds, nor were temperatures below T_{ice} observed. This provides
1134 strong additional observational support for the conclusions by Drdla et al. (2003), Larsen et al.
1135 (2004), Pagan et al. (2004), Voigt et al. (2005), Pitts et al. (2011), and Hoyle et al. (2013) that
1136 NAT clouds can form without the prior formation of ice clouds. Since laboratory experiments
1137 suggest that homogenous freezing of NAT is unlikely, a possible mechanism of ice-free
1138 formation of NAT could be heterogeneous nucleation on solid particulates such as meteoritic
1139 dust (Voigt et al., 2005; Hoyle et al., 2013), although Biermann et al. (1996) suggested that
1140 heterogeneous reaction rates on micrometeorites are too low. When the airmass temperature
1141 dropped rapidly due to adiabatic cooling, STS PSCs formed first when the temperature
1142 decreased below approximately $T_{\text{NAT}} - 4$ K. If the temperature further decreased below T_{ice} ,
1143 ice PSCs were formed. Then when the airmass temperature started to increase above T_{ice} ,
1144 NAT/STS mixture PSCs were formed, as suggested by the formation pathway of NAT clouds
1145 from ice clouds (e.g. Carslaw et al., 1995).

1146 We further analysed the chlorine activation process based on MLS observations of HCl and
1147 ClO and the ATLAS Chemistry and Transport Model runs. Several sensitivity runs with
1148 different temperature histories ~~or different PSC types~~ were conducted. We find that our cases
1149 fall in one of two categories.

1150 (1) In most cases chlorine activation occurred sufficiently rapidly, such that the degree of
1151 chlorine activation by the first PSC encounter for the respective air mass was limited by the
1152 initially available ClONO₂, i.e. ClONO₂ concentrations fell to very low values. For these
1153 cases, ATLAS model results, i.e. the modelled mixing ratios of HCl and ClO_x before and after
1154 the chlorine activation by the PSCs, generally agreed well with the MLS observations. The
1155 good agreement is expected, since for these cases the degree of chlorine activation only

1156 depends on available ClONO₂ and is largely insensitive to the rate of the heterogeneous
1157 reactions and therefore to the exact PSC ~~composition and~~ temperature. ~~This finding is further~~
1158 ~~illustrated by the fact that all ATLAS sensitivity runs give very similar results for all these~~
1159 ~~cases.~~

1160 (2) In a few cases, temperatures during the first PSC encounter remained higher (around
1161 T_{NAT} – 4 K) and the chlorine activation is slower, such that the rates of the heterogeneous
1162 reactions integrated over the time of exposure to PSCs limit the degree of chlorine activation,
1163 rather than the available amount of ClONO₂. In these cases, substantial amounts of ClONO₂
1164 can survive the initial PSC encounter and the model is not always able to reproduce the
1165 degree of chlorine activation. ~~As expected for these cases, the ATLAS sensitivity runs show~~
1166 ~~that the amount of chlorine activation depends on both, PSC composition and temperature.~~ In
1167 particular, the sensitivity of chlorine activation to temperature is extremely large in these
1168 situations, suggesting that a temperature uncertainty of ±1 K is sufficient to explain the most
1169 discrepancies between ~~model modelled and measured HCl amount results and observations.~~
1170 However, based on the data from the winter 2009/2010 these situations are fairly rare. T_{NAT} –
1171 4 K is an approximate threshold temperature for rapid chlorine activation on PSCs.

1172

1173

1174 **Author Contribution**

1175 H. N. and M. T. designed the method of this study. I. W. developed and ran the ATLAS box
1176 model, ran trajectory calculations, and developed the PSC interpolation algorithm. T. W., M.
1177 C. P., and L. R. P. developed and analysed PSC observations from CALIPSO/CALIOP data.
1178 M. L. S. developed and analysed minor species from Aura/MLS data. H. N, I. W., R. L., and
1179 M. R. discussed on the analysis results. H. N. prepared the manuscript with contributions
1180 from all co-authors.

1181

1182

1183 **Acknowledgements**

1184 We acknowledge European Centre for Medium-Range Weather Forecasts (ECMWF) for
1185 providing us with the ERA Interim reanalysis data. We also acknowledge Atmospheric
1186 Chemistry and Dynamics Laboratory (Code 614) of Goddard Space Flight Center, National
1187 Aeronautics and Space Administration (NASA) for providing the MERRA annual minimum
1188 temperature to produce Figure 1. One of the authors (HN) appreciates the warm hospitality
1189 given by all the members of Alfred Wegener Institute for Polar and Marine Research at
1190 Potsdam, Germany when he was staying there for half a year as a sabbatical visit. Work at
1191 the Jet Propulsion Laboratory, California Institute of Technology, was done under contract
1192 with ~~the NASA National Aeronautics and Space Administration.~~
1193
1194

1195 **References**

1196

1197 Biermann, U. M., Presper, T., Koop, T., Mößinger, J., Crutzen, P. J., and Peter, Th.: The
1198 unsuitability of meteoritic and other nuclei for polar stratospheric cloud freezing,
1199 *Geophys. Res. Lett.*, 23, 1693-1696, 1996.

1200 Carslaw, K. S., Luo, B. P., Clegg, S. L., Peter, Th., Brimblecombe, P., Crutzen, P. J.:
1201 Stratospheric aerosol growth and HNO₃ gas phase depletion from coupled HNO₃ and
1202 water uptake by liquid particles, *Geophys. Res. Lett.*, 21, 2479-2482, 1994.

1203 Carslaw, K. S., Wirth, M., Tsias, A., Luo, B. P., Dörnbrack, A., Leutbecher, M., Volkert, H.,
1204 Renger, W., Bacmeister, J. T., Reimer, E., and Peter, Th.: Increased stratospheric ozone
1205 depletion due to mountain-induced atmospheric waves, *Nature*, 391, 675-678, 1998.

1206 Carslaw, K., Peter, T., and Müller, R.: Uncertainties in reactive uptake coefficients for solid
1207 stratospheric particles – 2. Effect on ozone depletion, *Geophys. Res. Lett.*, 24, 1747–1750,
1208 1997.

1209 Crutzen, P. J., and Arnold, F.: Nitric acid cloud formation in the cold Antarctic stratosphere: a
1210 major cause for the springtime 'ozone hole', *Nature*, 324, 651-655, 1986.

1211 Dee, D. P., Uppala, S. M., Simmons, A. J., Berrisford, P., Poli, P., Kobayashi, S., Andrae, U.,
1212 Balsameda, M. A., Balsamo, G., Bauer, P., Bechtold, P., Beljaars, A. C. M., van de Berg,
1213 L., Bidlot, J., Bormann, N., Delsol, C., Dragani, R., Fuentes, M., Geer, A. J., Haimberger,
1214 L., Healy, S. B., Hersbach, H., Hólm, E. V., Isaksen, L., Kållberg, P., Köhler, M.,
1215 Matricardi, M., McNally, A. P., Monge-Sanz, B. M., Morcrette, J.-J., Park, B.-K., Peubey,
1216 C., de Rosnay, P., Tavolato, C., Thépaut, J.-N., and Vitart, F.: The ERA-Interim
1217 reanalysis: configuration and performance of the data assimilation system, *Q. J. R.*
1218 *Meteorol. Soc.*, 137, 553–597, 2011.

1219 Dörnbrack, A., Pitts, M. C., Poole, L. R., Orsolini, Y. J., Nishii, K., and Nakamura, H.: The
1220 2009-2010 Arctic stratospheric winter – general evolution, mountain waves and
1221 predictability of an operational weather forecast model, *Atmos. Chem. Phys.*, 12, 3659-
1222 3675, doi:10.5194/acp-12-3659-2012, 2012.

- 1250 Drdla, K., and Schoeberl, M. R.: Microphysical modeling of the 1999-2000 Arctic winter, 2,
1251 Chlorine activation and ozone depletion-₂. J. Geophys. Res.₂ 108, 8319,
1252 doi:10.1029/2001JD001159, 2003.
- 1253 Drdla, K., Schoeberl, M. R., and Browell, E. V.: Microphysical modeling of the 1999-2000
1254 Arctic winter, 1, Polarstratospheric clouds, denitrification, and dehydration-₂. J. Geophys.
1255 Res.₂ 108, 8312, doi:10.1029/2001JD000782, 2003.
- 1256 Dye, J. E., Baumgardner, D., Gandrud, B. W., Kawa, S. R., Kelly, K. K., Loewenstein, M.,
1257 Ferry, G. V., Chan, K. R., and Gary, B. L.: Particle size distribution in Arctic polar
1258 stratospheric clouds, growth and freezing of sulfuric acid droplets, and implications for
1259 cloud formation, J. Geophys. Res., 30, 8015-8034, 1992.
- 1260 Farman, J. C., Gardiner, B. G., and Shanklin, J. D.: Large losses of total ozone in Antarctica
1261 reveal seasonal ClO_x/NO_x interaction, Nature, 315, 207-210, 1985.
- 1262 Hanson, D. and Mauersberger, K.: Laboratory studies of the nitric acid trihydrate:
1263 Implications for the south polar stratosphere, Geophys. Res. Lett., 15, 855-858, 1988.
- 1264 Hanson, D. R. and Ravishankara, A. R.: Reactive uptake of ClONO₂ onto sulfuric acid due to
1265 reaction with HCl and H₂O, J. Phys. Chem., 98, 5728–5735, 1994.
- 1266 Hoyle, C. R., Engel, I., Luo, B. P., Pitts, M. C., Poole, L. R., GroöB, J.-U., and Peter, T.:
1267 Heterogeneous formation of polar stratospheric clouds - Part 1: Nucleation of nitric acid
1268 trihydrate (NAT), Atmos. Chem. Phys., 13, 9577-9595, 2013.
- 1269 Iraci, L. T., Middlebrook, A. M., and Tolbert, M. A.: Laboratory studies of the formation of
1270 polar stratospheric clouds: Nitric acid condensation on thin sulphuric acid films, J.
1271 Geophys. Res.₂ 100, 20,969-20,977, 1995.
- 1272 Koop, T., Biermann, U. M., Raber, W., Luo B.P., Crutzen, P. J., and Peter, T.: Do
1273 stratospheric aerosol droplets freeze above the ice frost point? Geophys. Res. Lett.₂ 22,
1274 917-920, 1995.
- 1275 Koop, T., Carslaw, K. S., and Peter, T.: Thermodynamic stability and phase transitions of
1276 PSC particles, Geophys. Res. Lett.₂ 24, 2199-2202, 1997.

書式変

書式変

- 1277 Lambert, A., Santee, M. L., Wu, D. L., and Chae, J. H.: A-train CALIOP and MLS
1278 observations of early winter Antarctic polar stratospheric clouds and nitric acid in 2008,
1279 *Atmos. Chem. Phys.*, 12, 2899-2931, doi:10.5194/acp-12-2899-2012, 2012.
- 1280 Larsen, N., Knudsen, B. M., Rosen, J. M., Kjome, N. T., Neuber, R., and Kyrö, E.:
1281 Temperature histories in liquid and solid polar stratospheric cloud formation, *J. Geophys.*
1282 *Res.*, 102, 23,505-23,517, 1997.
- 1283 Larsen, N., Knudsen, B. M., Svendsen, S. H., Deshler, T., Rosen, J. M., Kivi, R., Weisser, C.,
1284 Schreiner, J., Mauerberger, K., Cairo, F., Ovarlez, J., Oelhaf, H., and Spang, R.:
1285 Formation of solid particles in synoptic-scale Arctic PSCs in early winter 2002/2003,
1286 *Atmos. Chem. Phys.*, 4, 2001-2013, 2004.
- 1287 Lehmann, R., von der Gathen, P., Rex, M., and Streibel, M.: Statistical analysis of the
1288 precision of the Match method, *Atmos. Chem. Phys.*, 5, 2713-2727, SRef-ID:1680-
1289 7324/acp/2005-5-2713, 2005.
- 1290 Livesey, N., Van Snyder, W., Read, W., and Wagner, P.: Retrieval algorithms for the EOS
1291 Microwave Limb Sounder (MLS), *Geoscience and Remote Sensing, IEEE Transactions*,
1292 44, 1144-1155, doi:10.1109/TGRS.2006.872327, 2006.
- 1293 Livesey, N. J., Read, W. G., Froidevaux, L., Lambert, A., Manney, G. L., Pumphrey, H. C.,
1294 Santee, M. L., Schwartz, M. J., Wang, S., Cofield, R. E., Cuddy, D. T., Fuller, R. A.,
1295 Jarnot, R. F., Jiang, J. H., Knosp, B. W., Stek, P. C., Wagner, P. A., and Wu, D. L.:
1296 Version 3.3 and 3.4 Level 2 data quality and description document, D-33509, Jet
1297 Propulsion Laboratory, <http://mls.jpl.nasa.gov/>, 2013.
- 1298 Marti, J. and Mauersberger, K.: A survey and new measurements of ice vapour pressure at
1299 temperatures between 170 and 250 K, *Geophys. Res. Lett.*, 20, 363-366, 1993.
- 1300 Molina, L. T., and Molina, M. J.: Production of Cl₂O₂ from the self-reaction of the ClO
1301 radical, *J. Phys. Chem.*, 91 (1987), 433-436.
- 1302 Müller, R., Peter, Th., Crutzen, P. J., Oelhaf, H., Adrian, G. P., v. Clarmann, Th., Wegner, A.,
1303 Schmidt, U., and Lary, D.: Chlorine chemistry and the potential for ozone depletion in the
1304 arctic stratosphere in the winter of 1991/92, *Geophys. Res. Lett.*, 21, 1427-1430, 1994.

- 1334 Pagan, K. L., Tabazadeh, A., Drdla, K., Hervig, M. E., Eckermann, S. D., Browell, E. V.,
1335 Legg, M. J., and Foschi, P. G.: Observational evidence against mountain-wave generation
1336 of ice nuclei as a prerequisite for the formation of three solid nitric acid polar
1337 stratospheric clouds observed in the Arctic in early December 1999, *J. Geophys. Res.*,
1338 109, D04312, doi:10.1029/2003JD003846, 2004.
- 1339 Peter, T., and Groöß, J.-U.: Polar Stratospheric Clouds and Sulfate Aerosol Particles:
1340 Microphysics, Denitrification and Heterogeneous Chemistry, In: Müller, R. (ed.):
1341 Stratospheric Ozone Depletion and Climate Change, Royal Society of Chemistry, 2012.
- 1342 Pitts, M. C., Thomason, L. W., Poole, L. R., and Winker, D. M.: Characterization of Polar
1343 Stratospheric Clouds with spaceborne lidar: CALIPSO and the 2006 Antarctic season,
1344 *Atmos. Chem. Phys.*, 7, 5207-5228, 2007.
- 1345 Pitts, M. C., Poole, L. R., and Thomason, L. W.: CALIPSO polar stratospheric cloud
1346 observations: second-generation detection algorithm and composition discrimination,
1347 *Atmos. Chem. Phys.*, 9, 7577-7589, 2009.
- 1348 Pitts, M. C., Poole, L. R., Dörnbrack, A., and Thomason, L.W.: The 2009–2010 Arctic polar
1349 stratospheric cloud season: a CALIPSO perspective, *Atmos. Chem. Phys.*, 11, 2161–2177,
1350 2011.
- 1351 [Portmann, R. W., Solomon, S., Garcia, R. R., Thomason, L. W., Poole, L. R., and McCormick,](#)
1352 [M. P.: Role of aerosol variations in anthropogenic ozone depletion in the polar regions. *J.*](#)
1353 [Geophys. Res.](#), 101, 22,991-23,006, 1996.
- 1354 Sander, S. P., Abbatt, J., Barker, J. R., Burkholder, J. B., Friedl, R. R., Golden, D. M., Huie, R.
1355 E., Kolb, C. E., Kurylo, M. J., Moortgat, G. K., Orkin, V. L., and Wine, P. H.: Chemical
1356 kinetics and photochemical data for use in atmospheric studies, Evaluation Number 17,
1357 JPL Publication 10-06, Jet Propulsion Laboratory, California Institute of Technology,
1358 Pasadena, <http://jpldataeval.jpl.nasa.gov>, 2011.
- 1359 Solomon, S., Garcia, R. R., Rowland, F. S., and Wuebbles, D. J.: On the depletion of
1360 Antarctic ozone, *Nature*, 321, 755-758, 1986.
- 1361 [Solomon, S., Kinnison, D., Bandoro, J., and Garcia, R.: Simulation of polar ozone depletion:](#)
1362 [An update, *J. Geophys. Res.*, 120, 7958-7974, doi:10.1002/2015JD023365, 2015.](#)

書式変

書式変

- 1363 Voigt, C., Schreiner, J., Kohlmann, A., Zink, P., Mauersberger, K., Larsen, N., Deshler, T.,
1364 Kröger, C., Rosen, J., Adriani, A., Cairo, F., Di Donfrancesco, G., Viterbini, M., Ovarlez,
1365 J., Ovarlez, H., David, C., and Dörnbrack, A.: Nitric acid trihydrate (NAT) in polar
1366 stratospheric clouds, *Science*, 290, 1756-1758, 2000.
- 1367 Voigt, C., Schlager, H., Luo, B. P., Dörnbrack, A., Roiger, A., Stock, P., Curtius, J., Vössing,
1368 H., Borrmann, S., Davies, S., Konopka, P., Schiller, C., Shur, G., and Peter, T.: Nitric
1369 acid trihydrate (NAT) formation at low NAT supersaturation in polar stratospheric clouds
1370 (PSCs), *Atmos. Chem. Phys.*, 5, 1371-1380, 2005.
- 1371 Waters, J.W., Froidevaux, L., Harwood, R. S., Jarnot, R. F., Pickett, H. M., Read, W. G.,
1372 Siegel, P. H., Coeld, R. E., Filipiak, M. J., Flower, D. A., Holden, J. R., Lau, G. K.,
1373 Livesey, N. J., Manney, G. L., Pumphrey, H. C., Santee, M. L., Wu, D. L., Cuddy, D. T.,
1374 Lay, R. R., Loo, M. S., Perun, V. S., Schwartz, M. J., Stek, P. C., Thurstans, R. P.,
1375 Chandra, K. M., Chavez, M. C., Chen, G.-S., Boyles, M. A., Chudasama, B. V., Dodge,
1376 R., Fuller, R. A., Girard, M. A., Jiang, J. H., Jiang, Y., Knosp, B. W., LaBelle, R. C.,
1377 Lam, J. C., Lee, K. A., Miller, D., Oswald, J. E., Patel, N. C., Pukala, D. M., Quintero, O.,
1378 Scaff, D. M., Snyder, W. V., Tope, M. C., Wagner, P. A., and Walch, M. J.: The Earth
1379 Observing System Microwave Limb Sounder (EOS MLS) on the Aura satellite, *IEEE*
1380 *Transactions on Geoscience and Remote Sensing*, 44, 1075–1092, 2006.
- 1381 Wegner, T., Groß, J.-U., von Hobe, M., Stroh, F., Sumińska-Ebersoldt, O., Volk, C. M.,
1382 Hösen, E., Mitev, V., Shur, G., and Müller, R.: Heterogeneous chlorine activation on
1383 stratospheric aerosols and clouds in the Arctic polar vortex, *Atmos. Chem. Phys.*, 12,
1384 11095-11106, 2012.
- 1385 Winker, D. M., McGill, M., and Hunt, W. H.: Initial performance assessment of CALIOP,
1386 *Geophys. Res. Lett.*, 34, L19803, doi:10.1029/2007GL030135, 2007.
- 1387 Winker, D. M., Vaughan, M. A., Omar, A. H., Hu, Y., Powell, K. A., Liu, Z., Hunt, W. H.,
1388 and Young, S. A.: Overview of the CALIPSO mission and CALIOP data processing
1389 algorithms, *J. Atmos. Oceanic Technol.*, 26, 2310-2323,
1390 doi:10.1175/2009JTECHA1281.1, 2009.

1391 Wohltmann, I., Lehmann, R., and Rex, M.: The Lagrangian chemistry and transport model
1392 ATLAS: simulation and validation of stratospheric chemistry and ozone loss in the winter
1393 1999/2000, *Geosci. Model Dev.*, 3, 585–601, 2010.

1394 Wohltmann, I., Wegner, T., Müller, R., Lehmann, R., Rex, M., Manney, G. L., Santee, M. L.,
1395 Bernath, P., Suminska-Ebersoldt, O., Stroh, F., von Hobe, M., Volk, C. M., Hösen, E.,
1396 Ravegnani, F., Ulanovsky, A., and Yushkov, V.: Uncertainties in modelling
1397 heterogeneous chemistry and Arctic ozone depletion in the winter 2009/2010, *Atmos.*
1398 *Chem. Phys.*, 13, 3909–3929, 2013.

1399

1400

1401

1402 Table 1. List of the selected cases for the trajectory runs. The first column shows the ID
 1403 number of the case used in the following analysis, the second column shows the starting date,
 1404 and the third column the starting time of the trajectory. The remaining columns show the
 1405 location of the starting position (t=0) of the forward and backward trajectories.

1406

Case ID	Date	Time (UT)	latitude (N)	longitude (E)	altitude (km)	PT (K)	Pressure (hPa)
#01	2009/12/19	16:37:56	79.85	263.71	22.36	520.9	31.60
#02	2009/12/21	8:09:30	75.50	50.54	22.97	559.2	27.91
#03	2009/12/23	7:58:21	78.90	39.92	22.07	526.0	31.60
#04	2009/12/23	7:58:45	79.85	33.50	22.05	522.9	31.60
#05	2009/12/30	17:53:38	66.13	279.29	22.97	546.4	27.44
#06	2009/12/31	8:58:26	57.56	264.93	21.00	511.8	40.68
#07	2009/12/31	12:10:25	76.70	241.31	22.15	531.7	31.60
#08	2009/12/31	16:59:14	70.28	288.19	24.05	565.3	22.61
#09	2009/12/31	18:35:15	60.44	273.13	24.95	612.4	19.84
#10	2010/1/1	9:39:12	66.12	260.59	22.97	551.0	27.60
#11	2010/1/1	17:41:15	66.12	282.38	24.05	570.7	23.24

1407

1408

1409

1410 **Figure Captions**

1411

1412 Figure 1. Variation of the minimum temperature (50-90°N) in the Arctic stratosphere at 30
1413 hPa by Modern Era Retrospective-Analysis (MERRA) data. The thick black line shows the
1414 average minimum temperature between 1978/79 and 2013/14, while the thick and thin shaded
1415 area represents 30-70% and 10-90% percentile distributions, respectively. The red line shows
1416 the minimum temperature in the 2009/2010 Arctic winter. Two horizontal green lines
1417 represent the Type I (NAT) PSC threshold temperature assuming 6 ppbv HNO₃ and 4.5 ppmv
1418 H₂O, and the Type II (ice) PSC frost point temperature, respectively.

1419

1420 Figure 2. CALIOP PSC field for 21 December 2009 (a) and for 1 January 2010 (b) at the 550
1421 K potential temperature surface. The green area represents STS PSCs, the red area mixed
1422 NAT and STS PSCs, and the blue area ice PSCs. Grey and black circles show CALIOP
1423 observation points for nighttime orbit segments. No measurements are available in the grey
1424 area around the pole (>82°N) due to the orbital coverage of the CALIPSO satellite.

1425

1426 Figure 3. (a) Time-altitude plot of the PSC distribution on 21 December 2009 from 13.09 to
1427 13.30 UTC (fractional hours). PSC classifications are color coded (STS, M1: Mix 1, M2:
1428 Mix 2, M2e: Mix 2 enhanced, Ice, IceW: Wave Ice, for details see (Pitts et al., 2011)). The
1429 labels on the horizontal axis show fractional time, latitude and longitude. The cross with “n1”
1430 denotes the starting point of the forward/backward trajectories of panels (b) and (c) where mix
1431 1 PSC was present. (b) HCl measurements by MLS (green dots with error bars) along 5 day
1432 forward and 5 day backward trajectories starting at the cross in panel (a). The match radius
1433 between MLS measurements and the trajectory is 200 km. The color coded areas show PSC
1434 occurrence measured by CALIOP along the trajectories, with the same color code as in
1435 Figure 2. Time is given relative to the trajectory starting time. (c) Temperature along the
1436 trajectories (blue line). The thin black lines show the threshold temperature for NAT
1437 formation T_{NAT} and $T_{\text{NAT}} - 3$ K. The thin blue line shows T_{ice} .

1438

1439 Figure 4. Same as Figure 3 but for 2 January 2010 from 3.63 to 3.82 UTC. The cross with
1440 “e4” denotes the starting point of forward/backward trajectories where mix 2 enhanced PSC
1441 was present.

1442

1443 Figure 5. Temperature along the trajectories for the cases #01 (a) started at 16:37:56 UT on
1444 19 December 2009 at altitude of 22.36 km, and, #04 (b) started at 07:58:21 UT on 23
1445 December 2009 at altitude of 22.05 km, as are ~~and #03 (c)~~ listed in Table 1. The color coded
1446 areas show PSC occurrence measured by CALIOP along the trajectories, with the ~~same~~ color
1447 code shown in lower left of panel (a), as in Figure 2. Shaded grey area represents that PSC
1448 types were unknown due to the CALIPSO orbital limitation ($>82^\circ$ N). The thin black lines
1449 show the threshold temperature for NAT formation T_{NAT} and $T_{\text{NAT}} - 3$ K. The thin blue line
1450 shows T_{ice} .

1451

1452 Figure 6. Same as Figure 5 but for trajectory cases ~~#0544~~ (a) started at 17:53:38 UT on 30
1453 December 2009 at altitude of 22.97 km, #06 (b) started at 08:58:26 UT on 31 December 2009
1454 at altitude of 21.00 km, and ~~#1105~~ (c) started at 17:41:15 UT on 1 January 2010 at altitude of
1455 24.05 km, respectively.

1456

1457 Figure 7. Same as Figure 5 but for trajectory cases ~~#078~~ (a) started at 12:10:25 UT on 31
1458 December 2009 at altitude of 22.15 km, ~~#087~~ (b) started at 16:59:14 UT on 31 December
1459 2009 at altitude of 24.05 km, and #10 (c) started at 09:39:12 UT on 1 January 2010 at altitude
1460 of 22.97 km, respectively.

1461

1462 Figure 8. Results of the ATLAS chemistry model along the trajectories and comparison with
1463 measurements by MLS for the trajectory case #03 starting ~~on 23 Dec. 2009~~ at 07:58:21 UT on
1464 23 December 2009 at altitude of 22.07 km. (a) Temperature (as in Figs. ~~ure~~ 5-7), (b) PSC
1465 surface area density, (c) ~~$\text{ClONO}_2 + \text{HCl}$ heterogeneous reaction rate~~, (d) HCl mixing ratio,
1466 (e) ClONO_2 mixing ratio, (f) ClO_x ($\text{ClO} + 2 \times \text{Cl}_2\text{O}_2$) ~~+ $2 \times \text{Cl}_2$~~ mixing ratio, (g) ClO
1467 mixing ratio, ~~(h) HNO_3 mixing ratio, and (i) O_3 mixing ratio~~. Matched MLS measurements of

1468 HCl ~~and~~, ClO, ~~HNO₃ and O₃~~ are shown in panels (~~cd~~) ~~and~~, (~~fg~~), (~~h~~) ~~and~~ (~~i~~) (green dots with
1469 error bars). Black line in pPanels (b) to (~~fi~~) show ATLAS model results. ~~of the ATLAS~~
1470 ~~chemistry model for the “STS+NAT” run (black curve), the “STS” run (grey curve) and the~~
1471 ~~“CALIPSO-constrained” run (blue curve).~~ The color coded areas show PSC occurrence
1472 measured by CALIOP along the trajectories, with the ~~same~~ color code shown in lower left of
1473 panel (b) as in Figure 2.

1474

1475 Figure 9. Same as Fig. ~~ure~~ 8 but for trajectory case #05 starting at 17:53:38 UT on 30
1476 December, 2009 ~~at 17:53:38~~ at altitude of 22.97 km. The orange dots in panels (~~cd~~) (~~fi~~)
1477 indicate the period of solar illumination when the solar zenith angle is smaller than 90 degrees.

1478

1479 Figure 10. Same as Fig. ~~ure~~ 8 but for trajectory case #08 starting at 16:59:14 UT on 31
1480 December, 2009 ~~at 16:59:14~~ at altitude of 24.05 km.

1481

1482 Figure 11. Same as Fig. ~~ure~~ 8 but for trajectory case #02 starting at 08:09:30 UT on 21
1483 December, 2009 ~~at 08:09:30~~ at altitude of 24.05 km.

1484

1485 Figure 12. Temperature sensitivity runs for trajectory case #02. The black line shows the
1486 standard ~~“STS+NAT”~~ run, the red line a sensitivity run with temperature increased by 1 K and
1487 the blue line a sensitivity run with temperature decreased by 1 K. MLS measurements and
1488 PSC types are the same as in Fig. ~~ure~~ 11.

1489

1490 Figure 13. Same as Fig. ~~ure~~ 8 but for trajectory case #09 starting at 18:35:15 UT on 31
1491 December, 2009 ~~at 18:35:15~~ at altitude of 24.95 km.

1492

1493 Figure 14. Temperature sensitivity runs for trajectory case #09. Line colors here are the same
1494 as those in Fig. 12.

1495

